Thermal-Piezoresistive Energy Pumps in Micromechanical Resonant Structures

Amir Rahafrooz, *Member, IEEE*, and Siavash Pourkamali, *Member, IEEE*

***Abstract*—The internal thermoelectromechanical transduction loop in micromechanical resonant structures has been studied in this work and utilized to electronically enhance their quality factor or generate spontaneous mechanical vibrations. Electrothermal force generation in a micromechanical structure can be coupled to the structural stress through piezoresistive effect. Under certain conditions (specially having a negative piezoresistive coefficient in n-type crystalline silicon), this could allow mechanical vibrations of the structure to feed from a dc bias current applied to the structure, forming an electromechanical energy pump. At lower dc bias currents, the mechanical energy generated by the pump can only compensate a portion of the mechanical losses of the resonant structure, leading to self-Q-enhancement, whereas at higher currents, it can fully compensate all the mechanical losses, leading to self-sustained oscillation. Extensional-mode dual-plate resonators with frequencies as high as 18.1 MHz were fabricated, and quality factor amplification was successfully demonstrated for such. The ability of such resonators to initiate and maintain self-sustained oscillations under both vacuum and atmospheric pressures has also been demonstrated. Frequencies as high as 19.4 MHz, output voltage peak-to-peak amplitudes as high as 825 mV, and power consumptions as low as a few milliwatts have been demonstrated for such self-sustained oscillators.**

***Index Terms*—Active resonator, electromechanical energy pump, microelectromechanical systems (MEMS) oscillator, MEMS resonator, piezoresistive readout, quality factor enhancement, self-oscillation, thermal actuation.**

I. Introduction

THERMAL actuation is one of the most conveniently implementable mechanisms widely used in microelectromechanical systems (MEMS) [1], [2]. Operation of such actuators is typically based on thermal expansion through Joule heating upon passing a current through an actuator element.

The secondary effect, which is the basis of this work, is that the resulting structural mechanical stress can change the electrical resistance of the actuator element due to the piezoresistive effect. A change in resistance, in turn, changes the amplitude of the generated heat and the resulting actuation force. This sequence of interrelated effects forms an internal thermoelectromechanical feedback loop. Depending on the existing phase shift in such feedback loop, it can either pump some additional energy into the mechanical motion of the structure or take some energy out of it. Such internal feedback mechanism is equivalent to having an electronic amplifier integrated within the structures, making such resonators active devices capable of signal amplification, Q-amplification, or even self-sustained oscillation by compensating mechanical structural losses.

In a resonant structure, when the pumped energy is in phase with mechanical vibration, with smaller feedback loop gain, only a portion of the mechanical losses can be compensated. This results in an electronic amplification of the resonator quality factor to effective resonator Q values much higher than the mechanical limits imposed by different loss mechanisms such as viscous damping [3], thermoelastic dissipation [4], [5], and anchor loss [6], as well as the intrinsic limit on the maximum achievable frequency, quality factor $(f \cdot Q)$ product which is intrinsic to the structural material [7], [8]. Such resonators with extremely high quality factors can enable implementation of ultranarrow-band RF filters, e.g., for direct channel selection in wireless communication.

At feedback loop gains of one and larger, the thermal-piezoresistive pump fully compensates the mechanical losses of the resonant structure, leading to self-sustained oscillation. Such self-sustained thermal-piezoresistive oscillators can be utilized as low-cost and compact frequency references. They can also be used individually or in large arrays of resonant mass sensors without the need for any external amplification circuitry.

Examples of similar self-sustained oscillations at microscale include actuation of micromechanical resonators with a constant air flow [9] or a laser [10], electron beam exposure of nanocantilevers [11], and oscillation based on a self-sustained vibrating-body field-effect transistor [12].

Self-oscillation of lower frequency flexural-mode thermal-piezoresistive resonators using thermal-piezoresistive energy pumps has been recently demonstrated in [13]. This work demonstrates the thermal-piezoresistive energy pumps and Q-enhancement as well as self-sustained oscillations resulting from such in higher frequency extensional-mode resonant structures.

II. Device Structure and Concept

Fig. 1 shows the in-plane mode shape of a dual-plate resonant structure used in this work. In this mode, the two plates move back and forth, while the two thermal actuators connecting them periodically extend and contract. Fig. 2 shows a schematic

Manuscript received January 23, 2012; revised June 20, 2012; accepted August 23, 2012. Date of publication September 21, 2012; date of current version November 16, 2012. The review of this paper was arranged by Editor A. M. Ionescu.

A. Rahafrooz is with the Department of Electrical and Computer Engineering, University of Denver, Denver, CO 80210 USA (e-mail: amir.rahafrooz@du.edu).

S. Pourkamali is with the Department of Electrical Engineering, The University of Texas at Dallas, Richardson, TX 75080 USA (e-mail: siavash.pourkamali@utdallas.edu).

Color versions of one or more of the figures in this paper are available online at http://ieeexplore.ieee.org.

Digital Object Identifier 10.1109/TED.2012.2215863

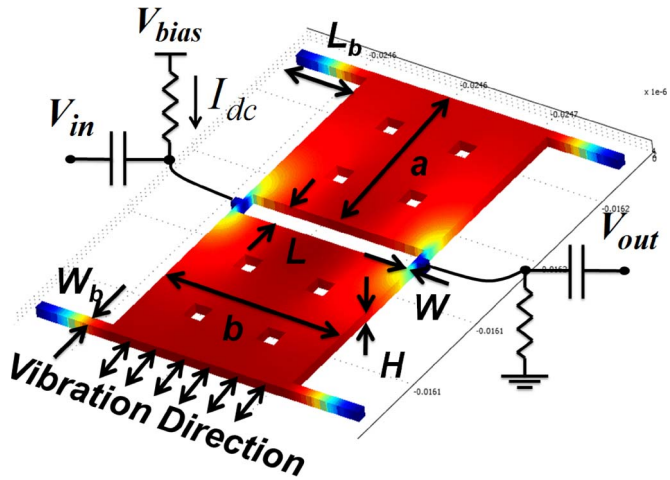

Fig. 1. COMSOL finite-element modal analysis of the in-plane extensional resonant mode of a dual-plate 4.5-MHz resonator and the used one-port electrical measurement configuration. Red and blue show the maximum and minimum vibration amplitudes, respectively.

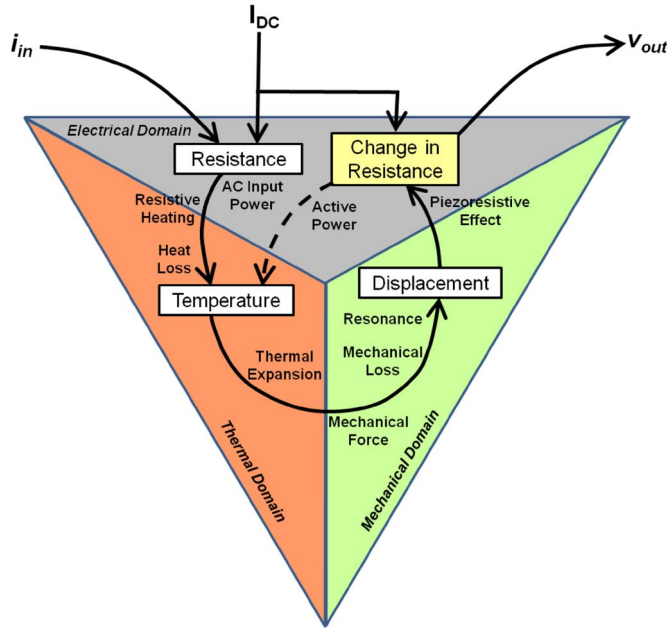

Fig. 2. Schematic diagram of a thermal-piezoresistive resonator showing the interaction between the three physical domains of electrical, thermal, and mechanical. It demonstrates how internal positive feedback loop can lead to self-Q-enhancement.

diagram, demonstrating the series of events involved in resonator transduction. To actuate the resonator, a combination of ac and dc currents is applied across the two terminals of the resonator. The resulting ohmic loss $P = R(I_{\rm dc} + i_{\rm ac})^2$ will have two ac components at f_0 and $2f_0$ in addition to its dc component, where f_0 is the frequency of the applied ac voltage. Due to the higher resistance of the narrow actuator beams in the middle of the structure, most of the ohmic loss occurs in the actuator beams. The alternating ohmic loss leads to temperature fluctuations in the narrow beams. The temperature fluctuations, in turn, result in a periodic extensional mechanical force in the actuators due to thermal expansion. Such force can actuate the resonator in its in-plane extensional mode if $f_0 = f_m$ or $f_0 = f_m/2$, where f_m is the mechanical resonance frequency

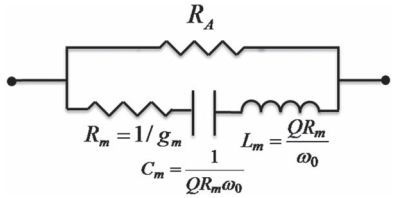

Fig. 3. Overall equivalent electrical circuit for one-port thermally actuated resonators with piezoresistive readout. R_A is the electrical resistance of the actuators.

of the in-plane mode. At resonance, the amplified vibration amplitude of the structure results in significant stress and strain in the actuator beams, which leads to modulation of the actuator beam electrical resistance due to the piezoresistive effect. Modulation of the resistance under a bias current $(I_{\rm dc})$ results in a measurable fluctuating output voltage that indicates the resonance amplitude and serves as the resonator output signal.

A. Q-Enhancement

Apart from the regular operation of thermal-piezoresistive resonators, periodic actuator resistance changes affect the periodic structural Joule heating. Therefore, they apply changes to the temperature fluctuations and actuation force of the resonator. The amplitude of this additional alternating heat component is given by $P_a = \Delta R \cdot I_{\rm dc}^2$, where ΔR is the amplitude of the periodic changes in the actuator resistance. The frequency of this added heat component is the same as both the mechanical vibrations of the resonator and the heat component that actuates it at the first place. Depending on the phase of ΔR, this heat component could add to or subtract from the actuating heat component. Mechanical vibrations of the resonator are out of phase (180° lagging behind the actuating heat power) due to 90° thermal lag in addition to a 90° mechanical lag [2]. For positive piezoresistive coefficients, ΔR will have the same phase as the resonator mechanical vibrations opposing the heat component actuating the resonator. In other words, this heat component maximizes when the resonator is at its most extended state. That is exactly the point where the input ac current and, therefore, the heating power should have been minimized, forcing the resonator to contract. This counteracting heat component limits the resonator vibration amplitude and acts as a negative feedback. This effect was used in [13] to suppress spurious vibrations of a flexural-mode micromechanical structure due to thermal noise, hence lowering its effective temperature (cooling) in that specific resonant mode.

For a structural material with negative longitudinal piezoresistive coefficient however, the generated heat component due to resistance modulation adds up to the heat component actuating the structure [14]. This effect can be formulated and discussed analytically using the resonator electrical equivalent circuit. Fig. 3 shows the equivalent electrical circuit for thermal-piezoresistive resonators derived in [2]. The model includes a resistor connecting the two terminals of the device that represents the electrical resistance of the actuator beams of the resonator, in parallel with a series RLC representing the resonant behavior of the structure. The current passing through the RLC represents the resonator motional current. The motional

conductance for such devices, which is the ratio of the motional current to the actuation voltage, is given by [2]

$$g_m = 4\alpha E^2 \pi_l Q \frac{AI_{\rm dc}^2}{KLC_{\rm th}\omega_m} \tag{1}$$

where α, E, and π_l are the thermal expansion coefficient, Young modulus, and longitudinal piezoresistive coefficient of the structural material, respectively, A, L, and $C_{\rm th}$ are the cross-sectional area, length, and thermal capacitance of the thermal actuators, respectively, and Q, K, ω_m, and $I_{\rm dc}$ are the quality factor, mechanical stiffness, resonance frequency, and bias current of the resonator, respectively.

Based on (1), thermal-piezoresistive resonators can potentially have negative motional conductance provided that the piezoresistive coefficient (π_l) of the structural material is negative. Single-crystalline n-type silicon is a convenient and widely available structural material with negative piezoresistive coefficient [15]. Therefore, unlike passive piezoelectric and electrostatic micromechanical resonators with positive motional resistance/conductance, thermal-piezoresistive resonators are similar to transistors and can be active electronic devices. A negative resistance/conductance in electronics is equivalent to an active energy pump. Therefore, as opposed to the passive resonators that just lose energy through their mechanical structure as well as their electronic circuitry, such thermal-piezoresistive resonators can absorb some energy from a dc electrical source (similar to transistors) and feed it into their mechanical vibrations.

Based on (1), by increasing the dc bias current, the motional conductance increases with a square relationship. The increased motional conductance can compensate for a higher portion of the mechanical losses. Therefore, by increasing the current, the effective quality factor of such devices can increase to higher values well beyond the mechanical limits.

The increase in the effective quality factor of the resonator can be shown as a function of motional conductance: Quality factor is defined as the ratio between the energy stored (E_S) and released in the resonator in each cycle and the energy dissipated per cycle (E_D)

$$Q = 2\pi \frac{E_S}{E_D}. \tag{2}$$

Considering a series RLC circuit which is the equivalent circuit of a mechanical resonator, the maximum energy stored in the inductor (L_m) is

$$E_S = \frac{1}{2} L_m I_{\rm MAX}^2 \tag{3}$$

where $I_{\rm MAX}$ is the maximum current passing through the RLC. There is no energy stored in the capacitor at this instant because the capacitor voltage is zero. On the other hand, the energy lost in the circuit in every cycle is

$$E_D = \frac{\pi R_m I_{\rm MAX}^2}{\omega_m}. \tag{4}$$

By substituting (3) and (4) into (2), the mechanical quality factor of the resonator can be found as follows:

$$Q_m = \frac{\omega_m L_m}{R_m}. \tag{5}$$

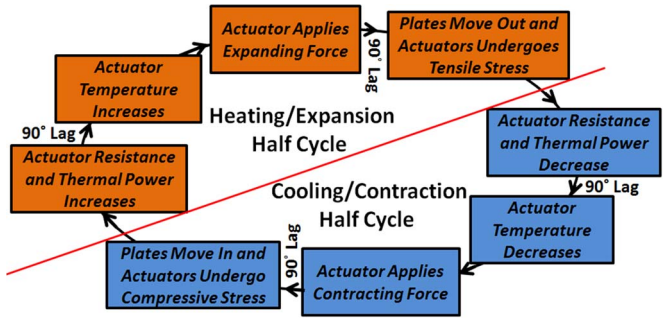

Fig. 4. Sequence of events causing an internal positive feedback loop that provides 360° of phase shift in thermal-piezoresistive resonators biased with a constant current that lead to self-sustained oscillation.

In order to find the effective quality factor of the thermal-piezoresistive resonators, the circuit in Fig. 3 can be used which consists of a series RLC in parallel with the physical resistance of the resonator. In this case, the stored energy is the same as that in the previous case. On the other hand, all the energy loss occurs in R_A and R_m. At resonance, the two resistors are in parallel. Therefore, the ratio of currents passing through them is inversely proportional to the ratio of their resistances. As a result, by knowing the current passing through R_m $(I_{\rm MAX})$, the overall energy loss per cycle can be calculated

$$E_D = \frac{\pi}{\omega_m}\left(R_m + \frac{R_m^2}{R_A}\right) I_{\rm MAX}^2. \tag{6}$$

By substituting (3) and (6) into (2), the effective quality factor can be found. By dividing both sides of the obtained equation by (5), the relationship between the mechanical and effective quality factors of a resonator can be derived

$$Q_{\rm eff} = \frac{Q_m}{1 + R_A \cdot g_m} \tag{7}$$

where Q_m and R_A are the mechanical quality factor and physical electrical resistance of the resonator, respectively. According to (7), for negative g_m values, the value of $Q_{\rm eff}$ can potentially be set to values orders of magnitude higher than the mechanical Q of the structure by tuning the value of g_m. This can be simply accomplished by tuning the bias current of the resonator.

B. Self-Sustained Oscillation

If the absolute value of the negative motional conductance resulting from negative piezoresistive coefficient is increased to reach and surpass the value of R_A^{-1}, the amount of energy absorbed from the dc source in each cycle surpasses the energy dissipated in the resonator. Therefore, instead of the resonator losing part of its overall energy in every cycle, it gains some additional energy in each cycle, which leads to instability of the resonant system and self-sustained oscillation [13], [16]. In this case, the resonator can maintain oscillation without the need for any external ac excitation and only based on the energy absorbed from the dc source. Similar to regular electronic oscillations, such oscillations are initiated by the existing thermal noise in the system.

Fig. 4 shows the sequence of physical phenomena leading to self-sustained oscillation. Upon application of a dc bias,

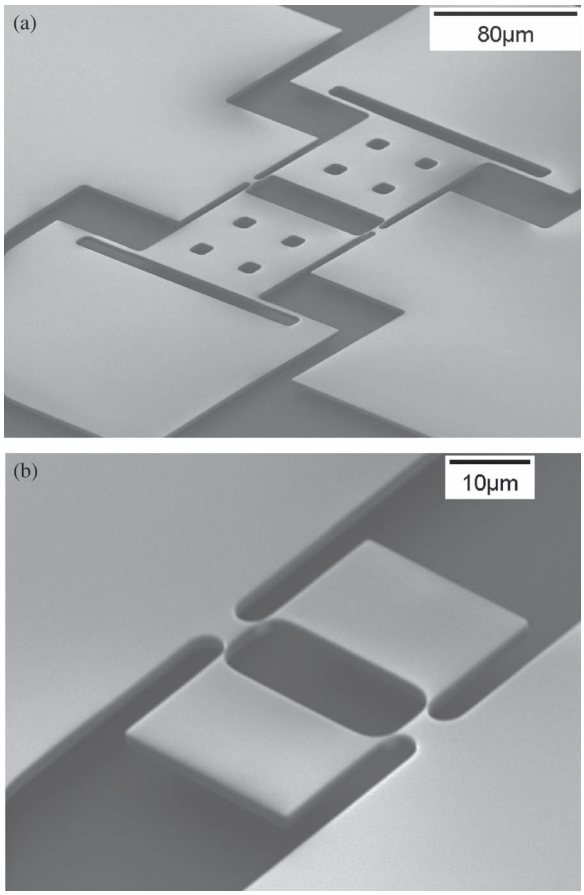

Fig. 5. SEM view of two fabricated 3.3-μm-thick n-type in-plane extensional-mode dual-plate resonators along 100 crystalline orientation of silicone with resonant frequencies of (a) 4.5 and (b) 18.1 MHz.

the thermal actuators heat up, pushing the plates further away from each other. Due to the mass (inertia) of the plates, the beams experience an overexpansion after pushing the plates and undergo tensile stress. Due to the negative piezoresistive coefficient, the tensile stress translates into reduced electrical resistance in the beams. Since a constant dc bias current is passing through the beams, this reduces their ohmic power and, therefore, their temperature, forcing them to contract. Again, due to the mass of the plates, the actuators experience over-contraction and undergo compressive stress, which increases their resistance. This increases the power consumption, forcing the structure to expand again. If the resulting driving force (due to heating and cooling) in each cycle is large enough to compensate for mechanical losses of the structure, the same sequence is repeated over and over in a self-sustained manner, and the vibration amplitude keeps increasing until it is limited by nonlinearities. Fig. 4 also shows how the thermal and mechanical delays provide an overall phase shift of 360° for the loop, leading to a perfect timing for the aforementioned sequence of physical phenomena to continue. The loop can be divided into two half cycles of heating and cooling.

III. Fabrication and Measurement Results

Fig. 5 shows the SEM view of two dual-plate resonators fabricated on a low-resistivity (0.01–0.05 $\Omega \cdot$ cm with a phosphorous concentration of 2.28×10^{17}–4.38×10^{18} cm^{-3}) n-type

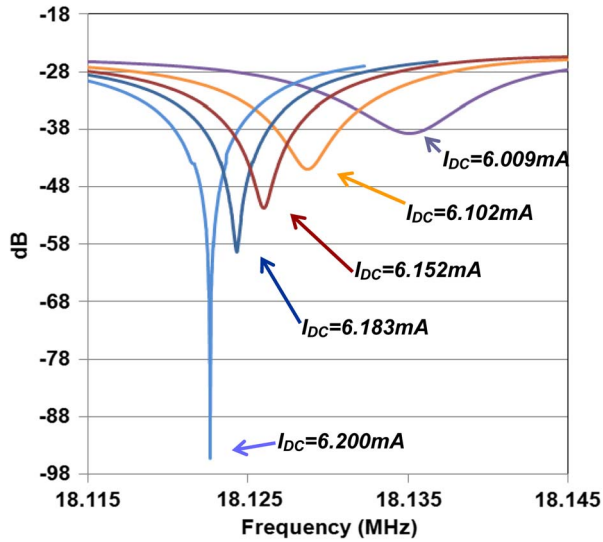

Fig. 6. Measured frequency response of the 18.1-MHz resonator in Fig. 5(b) under different dc bias currents directly taken from the network analyzer.

SOI substrate. The standard single-mask SOI-MEMS process [2] was used to fabricate the resonators in Fig. 5. A thin layer of silicon dioxide (∼200 nm thick) was first thermally grown on the substrate. The oxide was then patterned via photolithography and reactive-ion etching. The patterned silicon dioxide was then used as a hard mask to pattern the device layer using silicon deep reactive-ion etching. At the end, the structures were released in hydrofluoric acid (HF).

To minimize the resonator power consumptions and facilitate reaching high-enough motional conductances, the actuator beams were thinned down by thermal oxidation and subsequent oxide removal in hydrofluoric acid. The four support beams on the outer corners of the plates are to add to the vertical stiffness of the plates and avoid their stiction to the handle layer during HF release. In order to further minimize acoustic loss through the support beams and maximize resonator mechanical quality factors (Q), the dimensions of the beams are chosen so that their first flexural-mode frequency is close to the first in-plane extensional-mode frequency of the dual-plate resonator. The four openings in each of the plates in Fig. 5(a) are to expedite plate undercut in HF and avoid excessive undercut of the testing pads. To maximize the resonator transduction coefficients (motional conductance), the structures are aligned to the 100 crystal orientation, where the absolute value of the longitudinal piezoresistive coefficient is maximum [15].

The self-Q-enhancement capability of thermal-piezoresistive resonators was studied using the measurement configuration shown in Fig. 1. The applied dc bias currents were less than the oscillation threshold currents needed for initiating self-sustained oscillation. Fig. 6 shows the measured frequency responses for the 18.1-MHz resonator in Fig. 5(b) with different bias currents directly taken from the network analyzer. As the dc bias current of the resonator increases, the absolute value of the negative g_m increases, leading to a sharper decrease in conductance at resonance and, therefore, a higher effective quality factor. The measured resonance peaks are downward due to the negative piezoresistive coefficient of the structural material, resulting in a negative motional conductance. The

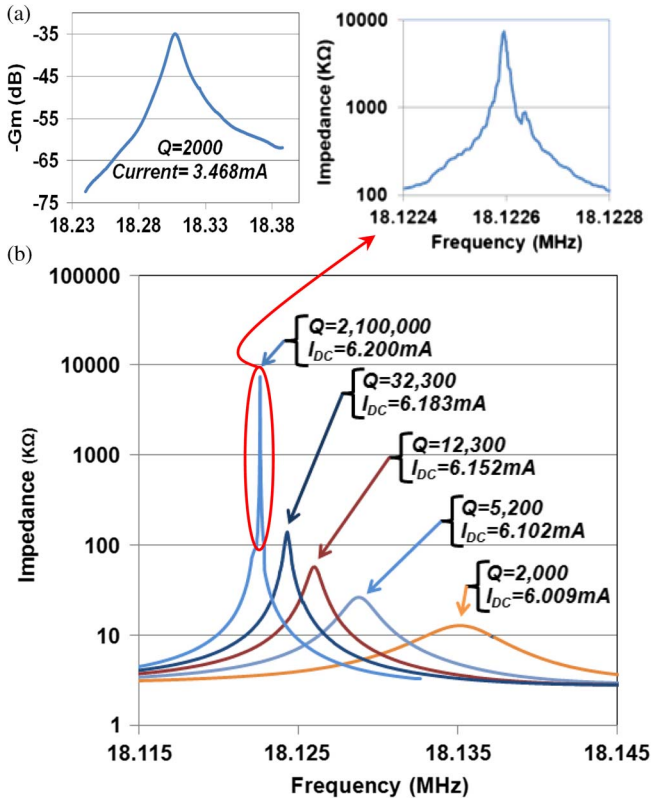

Fig. 7. (a) Frequency response of the 18.1-MHz resonator in Fig. 5(b) biased at a low bias current. The negative value of g_m is very small in this case, and the measured Q is the mechanical quality factor of the resonator. (b) Frequency responses for the same resonator at higher bias currents extracted from the measured plot in Fig. 6 showing significant Q-enhancement as the bias current increases.

negative motional conductance causes the motional current at resonance to be 180° out of phase with respect to the input ac actuation signal. Therefore, at resonance, the overall current passing through the resonator decreases, showing up as a downward peak (reduced transmission or increased equivalent impedance) in the frequency response.

Fig. 7(a) shows the frequency response of the absolute value of the motional conductance of the 18.1-MHz resonator at a low bias current of 3.468 mA extracted from the measured plot in Fig. 6. At this low current, the absolute value of g_m is very small, and the measured Q is equal to the mechanical Q of the resonator. At higher currents, the absolute value of g_m increases, leading to a sharper increase in the impedance of the structure at resonance. Fig. 7(b) shows the frequency plot of the overall resistance of the same resonator operating at higher bias currents, extracted from the measured frequency responses in Fig. 6. The upward frequency plots can be used to extract the resonator effective electrical Q. While the mechanical Q of the resonator measured at lower bias currents is only ~2000, the measured effective Q of the resonators increases sharply as the bias current increases above 6 mA and reaches ~2 100 000 with a bias current of 6.2 mA. The effective electrical Q has been calculated as the bandwidth in which the impedance decreases to half of its peak value divided by the resonance frequency.

Table I summarizes the measurement results obtained for both the 4.5- and 18.1-MHz dual-plate resonators in air,

TABLE I
MEASURED Q-ENHANCEMENT RESULTS FOR THE TWO 3.3-μm-THICK DUAL-PLATE RESONATORS IN FIG. 5 OPERATING IN AIR

Res. Dimensions (μm) a/b/L W/L_b / W_b	Current (mA)	Freq. (MHz)	Q_{eff} (×10^3)	Q_m R_A (KΩ)	$Z_{Res.}$ (KΩ)	Power (mW)
98/98/15.5 0.3/41.7/3.3	3.097	4.49813	4.60	4500 1.9	7.20	18.2
	3.304	4.49746	12.0		14.4	20.7
	3.403	4.49709	24.0		27.6	22.0
	3.443	4.49694	37.9		44.9	22.5
	3.484	4.49678	96.0		105	23.1
	3.504	4.49670	455		509	23.3
	3.507	4.49669	666		656	23.4
	3.509	4.49668	**1060**		**1130**	23.4
	3.511	4.49667	**40000**		**3985**	23.4
20/30/11.5 0.5/-/-	6.009	18.13500	2.00	2000 1.05	12.9	37.9
	6.102	18.12870	5.10		26.6	39.1
	6.152	18.12599	12.3		57.4	39.7
	6.162	18.12543	15.6		72.2	39.9
	6.174	18.12488	19.6		93.1	40.0
	6.183	18.12428	32.3		140	40.1
	6.192	18.12364	60.0		269	40.3
	6.197	18.12273	274		1060	40.3
	6.199	18.12271	**362**		**1760**	40.3
	6.200	18.12260	**2100**		**7490**	40.4

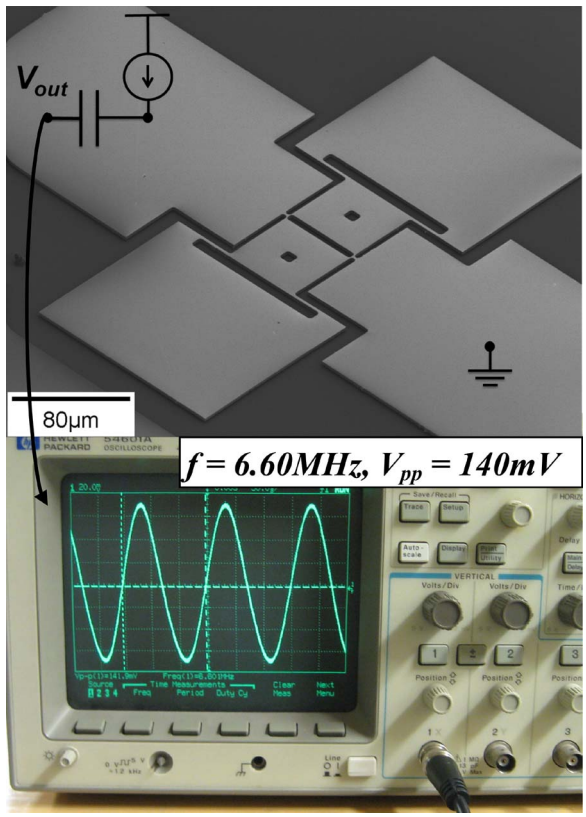

Fig. 8. SEM view and output signal shape of a 6.6-MHz 3.3-μm-thick n-type silicon thermal-piezoresistive dual-plate resonator capable of self-sustained oscillation. Only a dc bias current of 5.7 mA is being applied to the resonator (no amplifier), and the resonator is operating under atmospheric pressure.

showing significantly increased effective Q values as high as ~40 000 000 for the 4.5-MHz resonator.

Fig. 8 shows a similar resonator tested in a self-sustained oscillator configuration. A constant dc bias current has been applied to the resonator working in air without any amplifiers

TABLE II
MEASURED SELF-OSCILLATION RESULTS FOR DUAL-PLATE OSCILLATORS WITH DIFFERENT DIMENSIONS WHICH ARE SORTED BASED ON THEIR OSCILLATION FREQUENCIES

Resonator Dimensions (μm)							Freq. (MHz)	Oscillation Current (mA)	R_{DC} (KΩ)	$V_{P\text{-}PAC}$ (mV)	Power (mW)	V_{DC} (V)	Vibration Amplitude Vi_M (nm)	Pressure	$P_{AC\ out}$ / $P_{DC\ in}$ %
a	*b*	*L*	*W*	L_b	W_b	*H*									
97	97	27	~0.05	37	2.1	2	1.48	0.86	13.5	126	10.1	11.7	1.08	Vac.	2.69
198	198	16	~0.25	60	3.3	3.3	2.05	2.9	1.5	450	12.6	4.35	6.13	Air	25.8
98	98	16	~0.30	42	3.3	8.3	4.47	3.5	2	325	24.5	7	2.75	Vac.	11.6
98	98	16	~0.30	42	3.3	3.3	4.50	3.53	1.9	400	23.2	6.65	3.53	Air	15.0
67	67	17	~0.20	34	2.2	2	5.01	1.5	1.95	30	4.44	2.94	0.646	Vac.	2.55
67	67	27	~0.40	-	-	17	5.25	36	0.25	825	324	9	9.16	Air	22.9
								17		475	72.2	4.25	11.2	Vac.	27.9
68	68	10	~0.10	32	3.2	2	5.26	2.9	1.7	50	14.2	4.93	0.376	Vac.	2.54
68	68	16	~0.35	36	3.3	3.3	6.60	5.7	3.3	140	107	18.8	0.441	Air	1.86
67	67	17	~0.40	33	2.4	2	6.67	1.4	9.4	40	18.9	13.3	0.191	Vac.	0.75
20	30	11.5	~0.45	-	-	3.3	16.06	4.9	1.7	55	40.8	8.33	0.281	Air	1.65
20	30	11.5	~0.50	-	-	3.3	18.05	6.3	1.3	65	51.6	8.19	0.338	Air	1.98
20	30	11.5	~0.55	-	-	3.3	19.32	7.29	1.05	63	55.8	7.65	0.351	Air	2.06
							19.38	7.83		41	64.3	8.22	0.212	Vac.	1.25
							19.38	7.98		65	66.8	8.38	0.330	Vac.	1.94

or ac inputs involved. The ac-coupled output is ac coupled to the input of an oscilloscope. Relatively large resistors (five to ten times larger than R_A) were placed in series with the resonator to simulate a constant-current source. As the bias current increased at some point, the sinusoidal signal emerged on the oscilloscope. Further increase of the dc bias current increased the amplitude of the sinusoidal output waveform.

Table II summarizes the self-sustained oscillation measurement results for several tested dual-plate resonators with different dimensions under both vacuum and atmospheric pressures. At lower oscillation frequencies, air damping is the dominant source of energy loss; therefore, higher oscillation threshold currents are required in air than in vacuum. However, in the case of smaller resonators with higher oscillation frequencies, air damping becomes less dominant, and oscillation threshold currents are almost the same under both atmospheric and lower pressures. In order to have a better vision about the operation of the tested oscillators, their vibration amplitude (Vi_M) was also calculated. Knowing the resonator bias current and the piezoresistive coefficient, the vibration amplitude can be calculated as a function of the output voltage amplitude

$$Vi_M = \frac{V_{\rm ac} L}{2EV_{\rm dc}\pi_l} \tag{8}$$

where $V_{\rm ac}$ and $V_{\rm dc}$ are the ac and dc voltage amplitudes across the resonator, respectively. An estimated value of $\pi_l = 10^{-10}$ Pa^{-1} has been used to calculate the vibration amplitudes for all the measurements presented in Table II. Higher vibration amplitudes were shown for larger oscillators. It also demonstrates that, if such structures operate in vacuum, they can have larger vibration amplitudes by applying less dc bias currents. In order to further investigate the performance of the presented thermal-piezoresistive oscillators in Table II, the ratio of their output ac power $(P_{\rm ac\ out})$ to their input dc power $(P_{\rm dc\ in})$ was calculated as a measure of their efficiency. The change in this efficiency between different oscillators is believed to be mainly due to the fabrication-induced asymmetries and their different amounts of anchor loss.

IV. OSCILLATOR SCALING AND OPTIMIZATION

In order to optimize the presented fully micromechanical thermal-piezoresistive oscillators, one has to look at the oscillation condition for such devices. As discussed earlier, to achieve self-sustained oscillation, the resonator motional conductance should become larger in amplitude than the electrical conductance of the resonator $(g_m + R_A^{-1} < 0)$. By replacing the g_m from (1), this condition could be rewritten as follows:

$$P_{\rm dc} > \frac{KLC_{\rm th}\omega_m}{4\alpha E^2|\pi_l|QA} \tag{9}$$

where $P_{\rm dc} = R_A I_{\rm dc}^2$ is the dc power consumption of the resonator. From (9), the minimum required dc power consumption that can lead to self-oscillation could be found

$$P_{\rm dc_{Min}} = \frac{KLC_{\rm th}\omega_m}{4\alpha E^2|\pi_l|QA}. \tag{10}$$

One of the interesting aspects to look into is how the oscillation power requirement changes if the resonator dimensions are shrunk down to reach higher frequencies. If all resonator dimensions are scaled by a factor S, each of the parameters in (10) scales as follows: $K \propto S$, $C_{\rm th} \propto S^3$, $\omega_m \propto S^{-1}$, and $A \propto S^2$. Consequently, $P_{\rm dc_{Min}} \propto S^2$, meaning that, if the resonator is scaled down, the oscillation power requirement goes down with a square relationship.

Furthermore, it can be shown that, by keeping the size of the plates unchanged and only scaling down the dimensions of the thermal actuators, much lower oscillator dc power consumptions can be achieved. In this manner, the resonant frequency remains almost unchanged, and according to (10), if the actuator dimensions are scaled down by a scale factor of S, the minimum dc power consumption decreases with a square relationship ($P_{\mathrm{dc_{Min}}} \propto LA \propto S^3$).

V. Conclusion

It was demonstrated that the internal thermoelectromechanical interactions in microscale resonant structures could act as an energy pump absorbing power from a dc source and turning it into mechanical vibrations. In the case of n-type single-crystalline silicon structures, the output of this energy pump is in phase with the mechanical vibration of the structure, and its energy level is set by the passing dc bias current. At lower dc bias currents, the pumped mechanical energy can only compensate a portion of the mechanical losses of the structure, leading to self-Q-enhancement, whereas at higher currents, it can fully compensate all the mechanical losses, leading to self-sustained oscillation. Several of such resonant structures with different dimensions were characterized as both self-Q-enhanced resonators and self-sustained oscillators. Such devices have monolithic crystalline silicon structures and can be fabricated using a very simple CMOS-compatible process. In addition, in contrary to other types of MEMS filters and oscillators, the aforementioned mechanism could eliminate or minimize the need for external amplification circuitry. This decreases the required footprint and fabrication complexity for such devices. It is demonstrated that, by scaling down all the dimensions of such structures, their power consumption decreases with a square relationship.

Acknowledgment

The authors would like to thank Prof. Abdolvand, his research group members at Oklahoma State University, the staff at the Georgia Tech Nanotechnology Research Center, and Dr. A. Samarao for their help with silicon deep reactive-ion etching.

References

[1] D. Yan, A. Khajepour, and R. Mansour, "Design and modeling of a MEMS bidirectional vertical thermal actuator," *J. Micromech. Microeng.*, vol. 14, no. 7, pp. 841–850, Jul. 2004.

[2] A. Rahafrooz and S. Pourkamali, "High-frequency thermally actuated electromechanical resonators with piezoresistive readout," *IEEE Trans. Electron Devices*, vol. 58, no. 4, pp. 1205–1214, Apr. 2011.

[3] R. B. Bhiladvala and Z. J. Wang, "Effect of fluids on the Q factor and resonance frequency of oscillating micrometer and nanometer scale beams," *Phys. Rev. E*, vol. 69, no. 3, pp. 036307-1–036307-5, Mar. 2004.

[4] R. N. Candler, H. Li, M. Lutz, W.-T. Park, A. Partridge, G. Uama, and T. W. Kenny, "Investigation of energy loss mechanisms in micromechanical resonators," in *Proc. 12th Int. Conf. TRANSDUCERS*, Boston, Jun. 8–12, 2003, pp. 332–335.

[5] Y. B. Yi, A. Rahafrooz, and S. Pourkamali, "Modeling and testing of the collective effects of thermoelastic and fluid damping on silicon MEMS resonators," *J. Micro/Nanolith. MEMS MOEMS*, vol. 8, no. 2, pp. 023010-1–023010-7, Apr. 2009.

[6] V. Taş, S. Olcum, M. D. Aksoy, and A. Atalar, "Reducing anchor loss in micromechanical extensional mode resonators," *IEEE Trans. Ultrason., Ferroelectr., Freq. Control*, vol. 57, no. 2, pp. 448–454, Feb. 2010.

[7] V. B. Braginsky, V. P. Mitrofanov, and V. I. Panov, *Systems With Small Dissipation*. Chicago, IL: Univ. of Chicago Press, 1985.

[8] R. Tabrizian, M. Rais-Zadeh, and F. Ayazi, "Effect of phonon interactions on limiting the fQ product of micromechanical resonators," in *Proc. Int. Conf. TRANSDUCERS*, Denver, CO, Jun. 21–25, 2009, pp. 2131–2134.

[9] P. Neuzil, U. Sridhar, and B. Ilic, "Air flow actuation of micromechanical oscillators," *Appl. Phys. Lett.*, vol. 79, no. 1, pp. 138–140, Jul. 2001.

[10] K. Aubin, M. Zalalutdinov, T. Alan, R. B. Reichenbach, R. Rand, A. Zehnder, J. Parpia, and H. Craighead, "Limit cycle oscillations in CW laser-driven NEMS," *J. Microelectromech. Syst.*, vol. 13, no. 6, pp. 1018–1026, Dec. 2004.

[11] P. Vincent, S. Perisanu, A. Ayari, M. Choueib, V. Gouttenoire, M. Bechelany, A. Brioude, D. Cornu, and S. T. Purcell, "Driving self-sustained vibrations of nanowires with a constant electron beam," *Phys. Rev. B*, vol. 76, no. 8, pp. 085435-1–085435-5, Aug. 2007.

[12] D. Grogg, S. Ayoz, and A. M. Ionescu, "Self-sustained low power oscillator based on vibrating body field effect transistor," in *IEDM Tech. Dig.*, Dec. 7–9, 2009, pp. 1–4.

[13] P. G. Steeneken, K. Le Phan, M. J. Goossens, G. E. J. Koops, G. J. A. M. Brom, C. van der Avoort, and J. T. M. van Beek, "Piezoresistive heat engine and refrigerator," *Nat. Phys.*, vol. 7, no. 4, pp. 354–350, Apr. 2011.

[14] A. Rahafrooz and S. Pourkamali, "Active self-Q-enhancement in high frequency thermally actuated M/NEMS resonators," in *Proc. 24th IEEE MEMS*, Cancun, Mexico, Jan. 2011, pp. 760–763.

[15] A. A. Barlian, W. T. Park, J. R. Mallon, J. A. J. Rastegar, and B. L. Pruitt, "Fabrication review: Semiconductor piezoresistance for microsystems," *Proc. IEEE*, vol. 97, no. 3, pp. 513–552, Mar. 2009.

[16] A. Rahafrooz and S. Pourkamali, "Fully micromechanical piezo-thermal oscillators," in *IEDM Tech. Dig.*, 2010, pp. 7.2.1–7.2.4.

Amir Rahafrooz (S'07–M'11) received the Ph.D. degree from the University of Denver, Denver, CO.

He is currently an Associate Research Scientist with the Department of Electrical and Computer Engineering, University of Denver.

Siavash Pourkamali (S'02–M'06) received the M.S. and Ph.D. degrees from the Georgia Institute of Technology, Atlanta.

He is currently an Associate Professor of electrical engineering with The University of Texas at Dallas.